

Photophysical Properties of Oligophenylene Ethynylenes Modified by Donor and/or Acceptor Groups

Yoshihiro Yamaguchi,^{†,*} Yukihiro Shimoi,^{‡,§} Takanori Ochi,[†] Tateaki Wakamiya,[†] Yoshio Matsubara,[†] and Zen-ichi Yoshida^{†,*}

Department of Chemistry, Faculty of Science and Engineering, Kinki University, 3-4-1 Kowakae, Higashi-Osaka, Osaka 577-8502, Japan, Nanotechnology Research Institute, National Institute of Advanced Industrial Science and Technology (AIST), 1-1-1 Umezono, Tsukuba, Ibaragi 305-8568, Japan, and National Institute for Nanotechnology, National Research Council of Canada, 11421 Saskatchewan Drive, Edmonton, Alberta, Canada T6G 2M9

Received: November 30, 2007; Revised Manuscript Received: March 11, 2008

To create highly fluorescent organic compounds in longer wavelength regions, and to gain physical chemistry insight into the photophysical characteristics, we investigated photophysical properties (Φ_f , λ_{em} , τ , λ_{abs} , ϵ , k_r , and k_d) and their controlling factor dependence of the following π -conjugated molecular rods consisting of *p*-phenyleneethynylene units modified by donor (OMe) and/or acceptor (CN): (1) side-donor modification systems (**SD** systems), (2) side-acceptor modification systems (**SA** systems), and (3) systems consisting of donor block and acceptor block (**BL** systems). As a result, very high Φ_f values (>0.95) were obtained for **BL** systems. Bathochromic shifts of λ_{em} in the same π conjugation length were largest for **BL** systems. Thus we succeeded in the creation of highly efficient light emitters in the longer wavelength region by block modification (e.g., $\Phi_f = 0.97$, $\lambda_{em} = 464$ nm for **BL-9**), contrary to expectation from energy gap law. Considerably intense solid emission ($\Phi_f \sim 0.5$) in the longer wavelength region (500–560 nm) was also found for **BL** systems, presumably because of molecular orientation that hinders the self-quenching of fluorescence in solids. From (1) a Lippert–Mataga plot, (2) density functional theory (DFT) and time-dependent DFT (TD-DFT) calculations, and (3) the positive linear relationship between the optical transition energy (ν_{em}) and the difference between the highest occupied molecular orbital of the donor and the lowest unoccupied molecular orbital of the acceptor (HOMO(D)–LUMO(A) difference), it is elucidated that the excited singlet (S_1) state of **BL** systems has a high charge transfer nature. The number (n) of energetically equivalent dipolar structure (EEDS) units in the oligoarylene ethynylenes is shown to be a measure of the effective π conjugation length in the S_1 state. The S_1 state planarity increases with n values of EEDS units and by the introduction of donor and/or acceptor groups. It is worth noting that the Φ_f values increase linearly with the n values of EEDS units.

1. Introduction

Recent progress in biological,¹ chemical,² and materials³ science utilizing organic fluorescent materials has resulted in the strong requirement for highly efficient fluorophores. However a general concept or method for the creation of highly fluorescent materials in a desired wavelength region has not been established yet, even though various attempts to achieve this goal have been made.⁴ Thus the development of a method for the creation of highly fluorescent materials should be an urgent and significant subject. For this purpose, we considered π -conjugated molecular rods consisting of *p*-phenylene ethynylene units, because a marked increase in both the emission efficiency and emission wavelength should be expected by side modification with appropriate groups. Here, we report fluorescence emission characteristics of the following rod-shaped π -conjugated carbon framework modified by donor and acceptor groups (see Figure 1): (1) the side-donor modification systems (**SD** systems),⁵ (2) the side-acceptor modification systems (**SA** systems),^{4a} and (3) the side-donor and acceptor modification systems of block type (**BL** systems).⁶ To disclose the marked effect of block modification

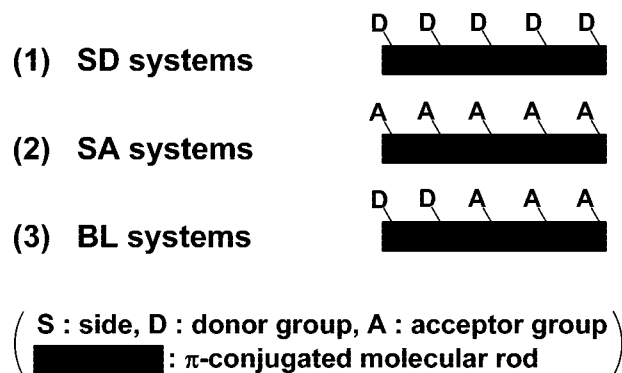


Figure 1. Side modification manner of π -conjugated molecular rods by donor and acceptor groups.

on the emission characteristics, our attention is focused on the electronic and spectral features (including solvent effect) arising from the block modification with donor and acceptor. A striking finding is presented concerning the linear relationship between the absolute quantum yield (Φ_f) and the number (n) of the energetically equivalent dipolar structure (EEDS) units in the excited singlet (S_1) state. This finding should be valuable for the creation of fluorophores with highly light-emitting efficiency.

2. Materials and Methods

2.1. Experimental Methods. UV–vis absorption spectra and fluorescence spectra measurements in spectral grade

* Corresponding author. Tel: +81-6-6721-2332; fax: +81-6-6723-2721; e-mail: yamaguch@chem.kindai.ac.jp (Y.Y.) and yoshida@chem.kindai.ac.jp (Z.-i.Y.).

[†] Kinki University.

[‡] National Institute of Advanced Industrial Science and Technology (AIST).

[§] National Institute for Nanotechnology (current address).

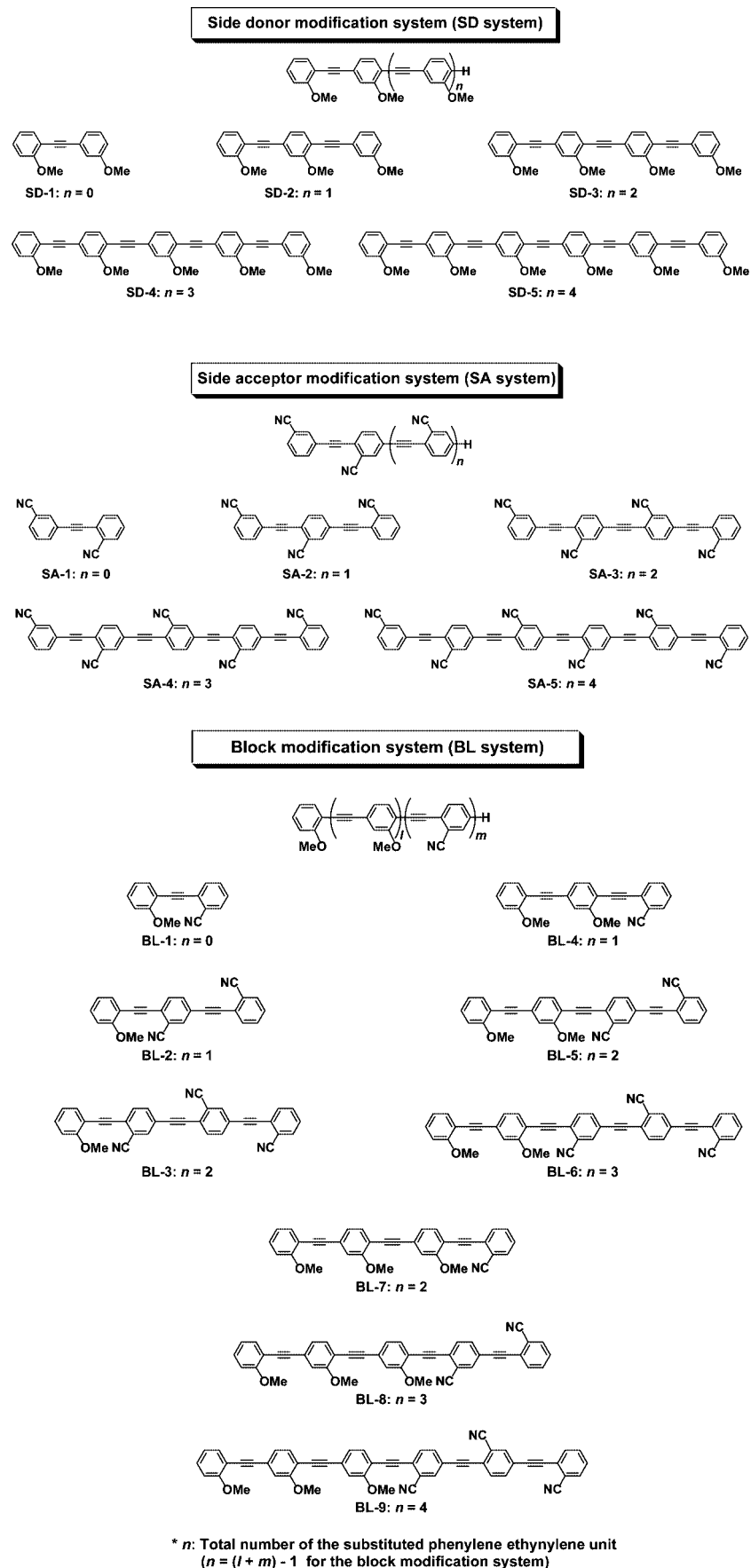


Figure 2. Structures of side-donor- and/or acceptor-modified phenylene ethynylene molecular rods.

solvents were performed with a Shimadzu UV-3100PC spectrometer and a Hitachi F-4500 spectrometer, respectively.

Absolute quantum yields (Φ_f) were determined by the Hamamatsu C9920-01 calibrated integrating sphere system.

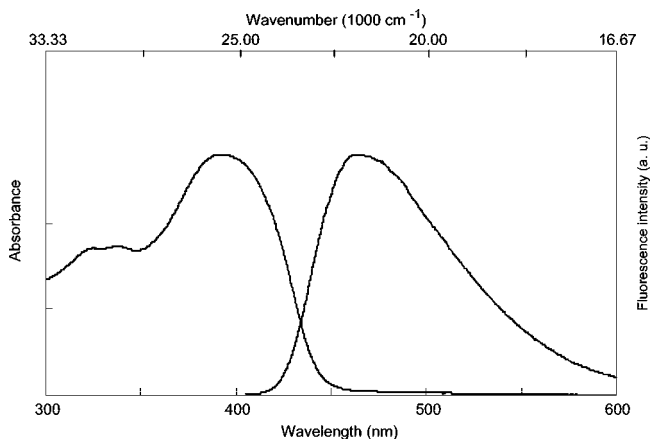


Figure 3. Absorption (left) and fluorescence (right) spectra of **BL-9** in chloroform.



Figure 4. Molecular orientation of **1** determined by X-ray analysis.

Time-resolved fluorescence spectra were measured by a Photon Technology International GL-3300 with a Photon Technology International GL-302 and a nitrogen laser/pumped dye laser system equipped with a four-channel digital delay/pulse generator (Stanford Research System, Inc. DG535) and a motor driver (Photon Technology International MD-5020). The excitation wavelength was 337 nm from a nitrogen laser without laser dye. The fluorescence lifetimes τ were

fitted by a single-exponential curve using a microcomputer. Freshly prepared 10-methylacridinium perchlorate was used to check the reliability of the measured τ value.⁷ To avoid oxygen quenching, bubbling argon in the solution and/or freeze-pump-thaw was performed immediately before the measurement of Φ_f and τ . ¹H and ¹³C NMR spectra were recorded on the Varian Mercury 300 spectrometer in CDCl₃ (300 MHz for ¹H, 75 MHz for ¹³C). Thin-layer chromatography (TLC) was performed on aluminum plates precoated with 0.25 mm thick silica-gel 60F₂₅₄ (Merck). Column chromatography was performed using silica gel (PSQ 100B, Fuji Silysia).

2.2. Calculation Methods. INDO/S. INDO/S calculation was carried out using the MOS-F V 4.2D program on the WinMOPAC system by Fujitsu, Inc. The structures calculated with MM2 were optimized by MOPAC 2000 V 1.3 (AM1 program).

Time-Dependent Density Functional Theory (TD-DFT). The DFT and TD-DFT calculations were performed using the Gaussian 03 package.⁸ The BHandHLYP hybrid functional was employed with the cc-pVDZ basis set. The geometries were fully optimized for the electronic ground states with “Opt(Tight)” and “Integral(Grid=UltraFine)” options. We examined the *cisoid* and *transoid* conformations for **SD-1**, **SA-1**, and **BL-1** (the *cisoid* means that both substituents in a diphenylacetylene unit are on the same side, and the *transoid* means that they are on the reverse side). The *cisoid* one is more stable in **SD-1** and **BL-1**, while the *transoid* one is more stable in **SA-1**, although the energy differences are quite small between the two conformations (see the Supporting Information). We imposed these conformations for the segments of **BL-2** to **BL-9** (see the molecular structures in Figures 2 and 6). In order to estimate the normalized CI coefficients accurately in the TD-DFT calculations, the threshold for printing them is set to be 10⁻⁶.

2.3. Molecular Design and Synthesis. In regards to the π -conjugated backbone of **SD**, **SA**, and **BL** systems, we considered oligophenylene ethynylenes that contain two to six benzene rings, respectively, as shown in Figure 2. Methoxy (MeO) group was selected as an electron-donating group for the side-donor modification and cyano (CN) group as an electron-

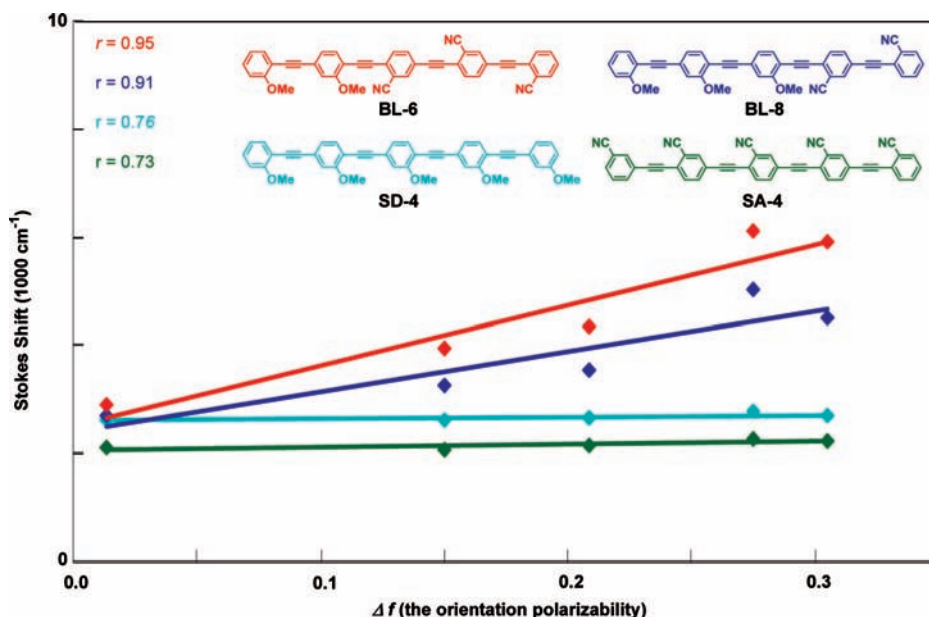


Figure 5. Lippert–Mataga plot for **SD-4**, **SA-4**, **BL-6**, and **BL-8**. Δf , the orientation polarizability, is defined by $\Delta f = (\epsilon - 1)/(2\epsilon + 1) - (n^2 - 1)/(2n^2 + 1)$ in eq 1. The colored points represent benzene, CHCl₃, THF, CH₃CN, and dimethylformamide (DMF) in the order of increasing Δf . Solvent properties (the values of dielectric constant (ϵ) and refractive index (n)) used to calculate Δf are available from Laurence’s paper.¹⁵

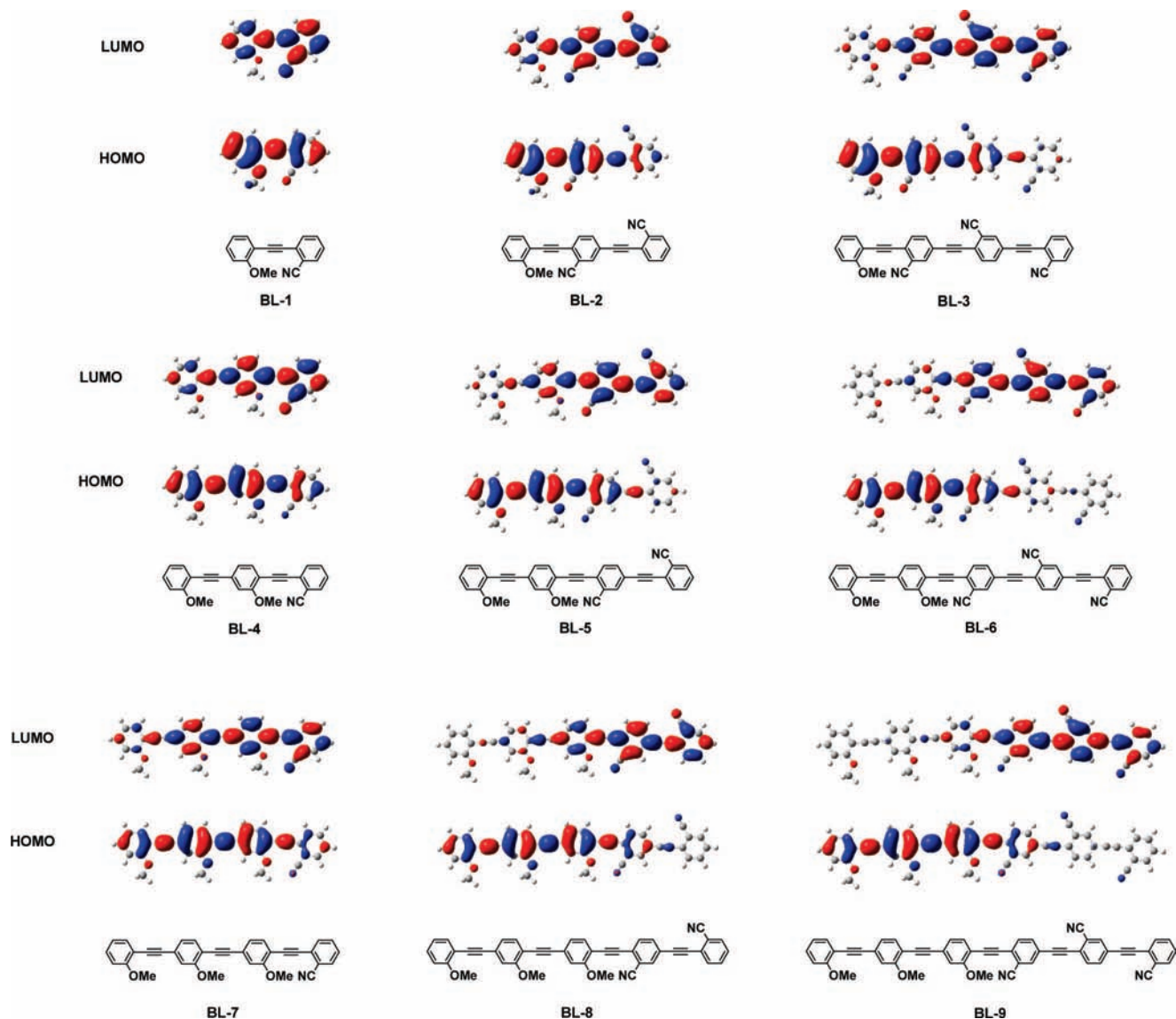


Figure 6. Molecular orbitals of BL systems by the DFT method. The upper ones represent the LUMOs, and the lower ones represent the HOMOs.

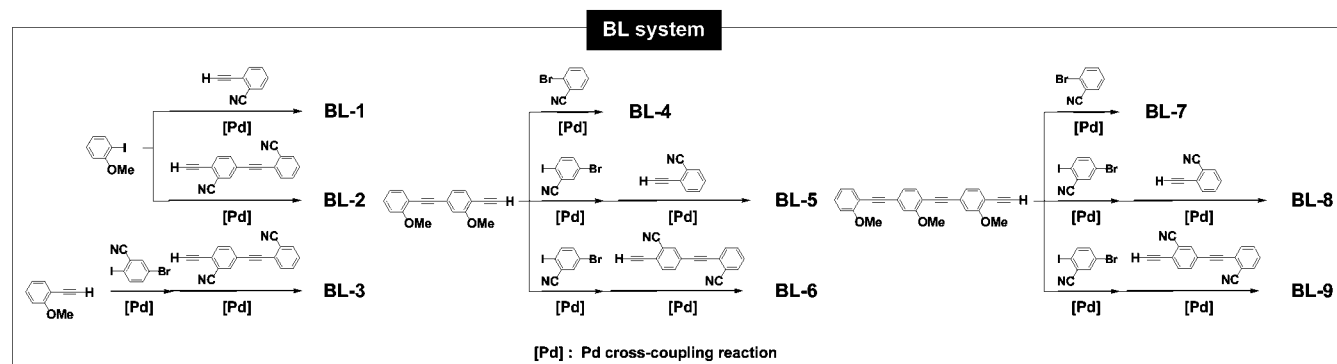
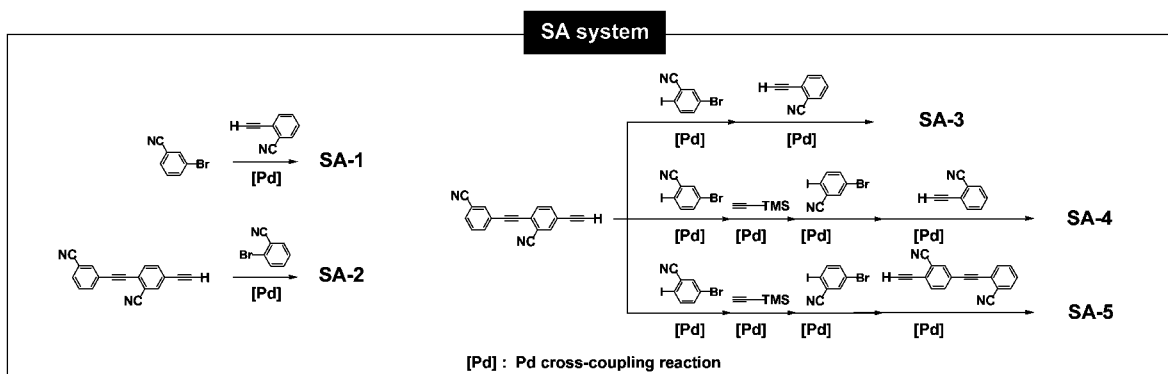
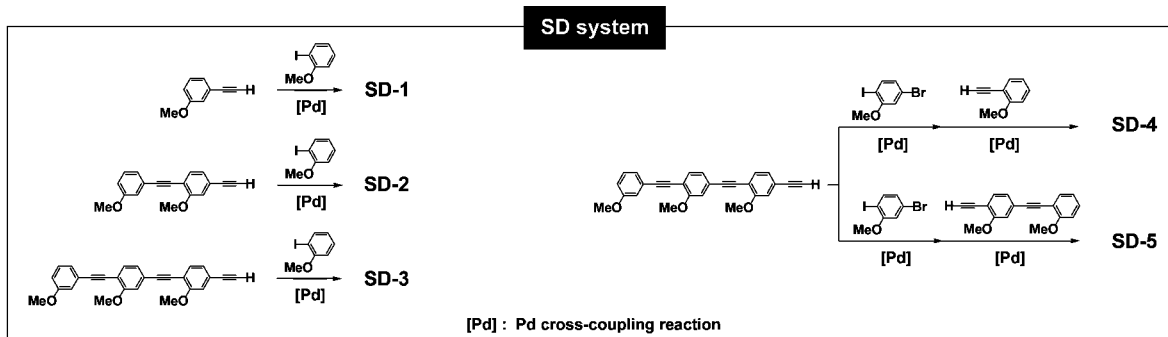
withdrawing group for side-acceptor modification, because of their stability to the employed various synthetic processes and the photostability of the final products.

Synthesis of SD, SA, and BL systems was carried out by repeating the Pd cross-coupling reaction,⁹ in which the reactivity difference between iodine and bromine on the same benzene ring is a key of the desired arrangement of the donor and acceptor units (Scheme 1). The general procedure for the Sonogashira cross-coupling reaction is as follows: A Schlenk flask charged with the halogen-derivative (1.0 equiv), Pd(Ph₃P)₂Cl₂ (0.1 equiv) and CuI (0.05 equiv) was evacuated and back-filled with Ar three times. Then dry Et₃N and tetrahydrofuran (THF) (2:1, v/v) was added to the flask. The mixture was stirred under Ar atmosphere at ambient temperature, then a solution of the acetylene-derivative (1.2 equiv) in dry THF was added successively. The reaction mixtures were stirred or refluxed under Ar atmosphere. The reaction was monitored by TLC. After the reaction was completed, the solvent was removed by a rotary evaporator, and the crude product was purified by column chromatography followed by recrystallization. The structures of SD, SA, and BL systems were confirmed by spectral data (¹H and ¹³C NMR spectroscopy and HR-FAB MS, see Supporting Information).¹⁰

3. Results and Discussion

3.1. Photophysical Properties. The photophysical properties of SD, SA, and BL systems and the parent systems (PR) together with radiative rate constant (k_r), radiationless rate constant (k_d), and emission lifetime (τ) are summarized in Table 1. Since the k_r and k_d are related to the corresponding emission quantum yields and lifetime by $\Phi_f = k_r \times \tau$ and $k_r + k_d = \tau^{-1}$, it is possible to calculate the values of k_r and k_d wherever quantum yield and lifetime data are available.¹¹ So far we reported^{4a-e} the fluorescence quantum yield values using quinine sulfate as the fluorescence standard, the τ values obtained from the absorption spectra, and the k_r and k_d values calculated from them. Strictly speaking, the emission characteristics should be discussed on the basis of the absolute quantum yield values, directly measured τ values, and the k_r and k_d values obtained from them (see Supporting Information), which are shown in Table 1. The Φ_f values obtained by both methods were close to each other, while the τ values obtained by both methods were not consistent. However the values of k_r/k_d calculated using the values of Φ_f and τ obtained by the method reported so far were completely identical to those calculated using the values of Φ_f and τ obtained by the present method.

SCHEME 1: Synthesis of SD, SA, and BL systems



As shown in Table 1, the τ values indicate that the emission of all compounds is typical fluorescence, and both the internal conversion (IC) and the intersystem crossing (ISC) to the triplet state become negligible with increase in n values judging from the Φ_f values (for $n \geq 1$). It is noted that the emission characteristics, particularly the quantum yield for all systems (**SD**, **SA**, **BL**, and **PR**), strikingly change between the $n = 0$ and $n = 1$ systems. A formal similarity is seen for *trans*-stilbene (Φ_f 0.04, $n = 0$) and *p*-distyrylbenzene (Φ_f 0.87, $n = 1$) reported by Saltiel et al.¹² and Sandros et al.,¹³ respectively, though it must be taken into account that the fluorescence of diphenylacetylene is due to the $S_2 \rightarrow S_0$ transition, but fluorescence of *trans*-stilbene is due to the $S_1 \rightarrow S_0$ transition.¹⁴ Interestingly, both λ_{em} and Φ_f values increase by the donor/acceptor modification and increase in the π conjugation length (n values). Thus very high Φ_f values (>0.95) at longer λ_{em} values (≥ 420 nm) are observed for the donor/acceptor modification system such as **SD-5** ($n = 4$), **BL-3** ($n = 2$), **BL-8** ($n = 3$), and **BL-9** ($n = 4$). It is worth noting that an increase in λ_{em} values and decrease in k_d values are found for all systems for $n \geq 1$, contrary to expectation from the so-called energy gap law.

Although the parent system (**PR-1–PR-4**) only emits in the UV region, this disadvantage was surmounted by the donor and/

or acceptor modification. Among them, the block modification was most effective for the bathochromic shift of the fluorescence maximum (λ_{em}) in the same π conjugation length (for example, in the case of $n = 2$: **BL-5** (434 nm) $>$ **BL-3** (419 nm) $>$ **BL-7** (407 nm) $>$ **SD-3** (397 nm) $>$ **PR-3** (389 nm) $>$ **SA-3** (388 nm)). Thus we succeeded in creating longer-wavelength light-emitters with high emission efficiency by the block modification of the longer π -conjugated backbones (e.g., $\Phi_f = 0.97$, $\lambda_{em} = 464$ nm for **BL-9** ($n = 4$), see Figure 3). The superiority in emission wavelength of **BL-9** over others can be explained by the smallest highest occupied molecular orbital (HOMO)/lowest unoccupied molecular orbital (LUMO) gap (largest λ_{abs} , Table 5) and the biggest Stokes shift (Table 1).

Interestingly, the values of λ_{em} for **BL** systems at the solid state were remarkably shifted to longer wavelength. On the other hand, the Φ_f value tends to decrease compared with that in solution. However, it is noted that **BL-3**, **BL-4**, **BL-6**, and **BL-8** are still intense ($\Phi_f = \text{ca. } 0.5$) fluorophores, even in solids, as shown in Table 2. Elucidation of the relationship between emission efficiency and molecular orientation in the solid state has not been accomplished because of the difficulty in obtaining the single crystals of

TABLE 1: The Photophysical Properties of SD, SA, and BL Systems and The Parent Systems (PR)^a in Chloroform^b

compound	<i>n</i>	Φ_f	λ_{em} (nm)	Stokes shift (nm)	$\log \epsilon$	λ_{abs} (nm)	τ (ns)	k_r (s ⁻¹)	k_d (s ⁻¹)
SD-1	0	0.23	331	20	4.31	311	6.17	3.73×10^7	1.25×10^8
SD-2	1	0.83	371	27	4.65	344	5.05	1.64×10^8	3.37×10^7
SD-3	2	0.94	397	37	4.75	360	4.14	2.27×10^8	1.45×10^7
SD-4	3	0.96	412	41	4.95	371	5.43	1.77×10^8	7.37×10^6
SD-5	4	0.97	420	40	5.13	380	4.55	2.13×10^8	6.59×10^6
SA-1	0	0.35	328	11	4.32	317	5.93	5.90×10^7	1.10×10^8
SA-2	1	0.83	363	24	4.69	339	4.28	1.94×10^8	3.97×10^7
SA-3	2	0.88	388	34	4.89	354	5.70	1.54×10^8	2.11×10^7
SA-4	3	0.90	402	31	4.94	371	4.59	1.96×10^8	2.18×10^7
SA-5	4	0.95	410	37	5.14	373	6.17	1.54×10^8	8.10×10^6
BL-1	0	0.44	374	47	4.40	326	5.86	7.51×10^7	9.56×10^7
BL-2	1	0.86	403	45	4.61	358	6.40	1.34×10^8	2.19×10^7
BL-3	2	0.95	419	49	4.87	370	4.93	1.93×10^8	1.01×10^7
BL-4	1	0.84	392	40	4.66	352	7.04	1.19×10^8	2.27×10^7
BL-5	2	0.93	434	54	4.81	380	5.36	1.74×10^8	1.31×10^7
BL-6	3	0.94	455	69	4.92	386	5.02	1.87×10^8	1.20×10^7
BL-7	2	0.95	407	42	4.90	365	4.73	2.01×10^8	1.06×10^7
BL-8	3	0.95	443	56	4.96	387	5.51	1.72×10^8	9.07×10^6
BL-9	4	0.97	464	72	4.99	392	5.31	1.83×10^8	5.65×10^6
PR-1	0	0.01	320	21	4.41	299	5.08	2.17×10^6	1.95×10^8
PR-2	1	0.83	348	20	4.59	328	5.51	1.51×10^8	3.09×10^7
PR-3	2	0.87	389	46	4.77	343	6.01	1.45×10^8	2.16×10^7
PR-4	3	0.93	389	35	5.13	354	6.27	1.48×10^8	1.12×10^7


^a Parent systems:  **PR-1: *n* = 0, PR-2: *n* = 1, PR-3: *n* = 2, PR-4: *n* = 3** ^b All spectra were measured at 295 K.

TABLE 2: Emission Characteristics of BL Systems In Solids (Powder)^a

compound	Φ_f^b	λ_{em} (nm)
BL-1	0.02	378
BL-2	0.02	477
BL-3	0.51	499
BL-4	0.49	515
BL-5	0.16	527
BL-6	0.48	562
BL-7	0.33	512
BL-8	0.46	532
BL-9	0.11	585

^a All spectra were measured at 295 K. ^b Absolute quantum yield (Φ_f) values were determined with a Hamamatsu C9920-01 calibrated integrating sphere system.

BL systems shown in Table 2. However Φ_f values of the donor /acceptor trisphenylene ethynylene (**1**) similar to BL systems were as follows: Φ_f of **1**, 0.87 in CHCl₃; 0.92 in polystyrene film; 0.90 in poly(methyl methacrylate) (PMMA) film; 0.36 in solids (powder); 0.11 in single crystals. From these data and the single crystal X-ray analysis data (see Figure 4), it is inferred that the decrease in Φ_f values in solids and in crystals seems to be due to self-quenching based on the face-to-face interaction (molecular orientation), where the face-to-face distance should play an important role for self-quenching. The Φ_f values also suggest that compound **1** is in a molecular disperse state in solution and in films. The data shown in Table 2 could be explained in the same way. Thus it is should be an attractive research subject to find out the conjugated π systems with high Φ_f values in solids and/or in crystals by controlling the molecular orientation (face-to-face interaction).

3.2. Electronic and Spectral Features of BL Systems.

Among the side modification systems, the BL system is of particular interest to investigate the S₁ state polarization due to the intramolecular charge transfer excitation. Thus we examined the solvent effect on photophysical properties of BL-6 and BL-8 as well as SD-4 and SA-4, which have almost the same molecular size. The results are summarized in Table 3.

TABLE 3: Effect of Solvent on Absorption and Fluorescence Characteristics of SD, SA, and BL Systems^a

compound	solvent	Φ_f^b	λ_{em} (nm)	Stokes		
				shift (nm)	$\log \epsilon$	λ_{abs} (nm)
SD-4	benzene	0.94	412	40	4.82	372
	CHCl ₃	0.93	411	40	4.86	371
	THF	0.97	409	40	4.86	369
	CH ₃ CN	0.95	407	40	4.88	367
	DMF	0.91	412	42	4.85	370
SA-4	benzene	0.99	403	32	4.74	371
	CHCl ₃	0.93	402	31	4.91	371
	THF	0.86	401	32	4.95	369
	CH ₃ CN	0.96 ^c	399	33	3.85 ^c	366
	DMF	0.89	404	34	4.72	370
BL-6	benzene	0.99	437	49	4.86	388
	CHCl ₃	0.96	455	69	4.87	386
	THF	0.88	459	76	4.90	383
	CH ₃ CN	0.67	482	107	4.91	375
	DMF	0.61	493	114	4.85	379
BL-8	benzene	0.99	432	45	4.89	387
	CHCl ₃	0.98	443	56	4.91	387
	THF	0.95	446	61	4.92	385
	CH ₃ CN	0.83	464	80	4.91	384
	DMF	0.72	468	89	4.85	379

^a All spectra were measured at 295 K. ^b For examination of solvent effect on quantum yield, we used quantum yield calculated relative to Quinine ($\Phi_f = 0.55$ in 0.1 M H₂SO₄), because the absolute quantum yields are shown to be very close each other. ^c These values are not optimized because of the very poor solubility of SA-4 in CH₃CN.

As shown in Table 3, almost no solvent effect is observed for the absorption and fluorescence spectra of SD and SA systems, and even for the absorption spectra of BL systems, while the fluorescence maxima (λ_{em}) of BL systems (BL-6 and BL-8) are shifted to considerably longer wavelengths as solvent polarity increases. Solvent effect on emission efficiency (Φ_f) is also quite contrastive between BL and other systems. Although the quantum yield of SD and SA systems is not altered with a change in the solvent polarity, that of BL systems remarkably decreases with an increase in the solvent polarity.

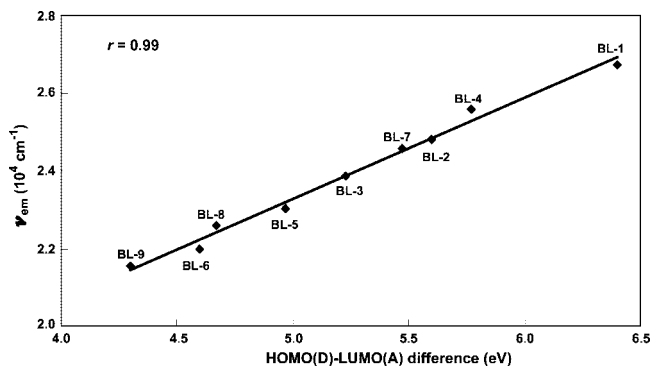


Figure 7. The relationship between the HOMO(D)–LUMO(A) difference calculated by TD-DFT and the ν_{em} of block systems (BL-1–BL-9).

TABLE 4: The Values of Slope (ρ) in a Lippert–Mataga Plot and the Relative Values of the Change in Dipole Moment ($\Delta\mu$) for SD-4, SA-4, BL-6 and BL-8

compound	ρ (the value of slope)	(ρ/ρ_{SD-3}) = the relative value of $\Delta\mu^2$	the relative value of $\Delta\mu$
SD-4	379	1.0	1.0
SA-4	523	1.4	1.2
BL-6	11282	29.8	5.5
BL-8	7395	19.5	4.4

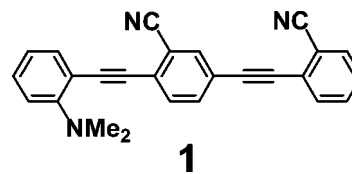
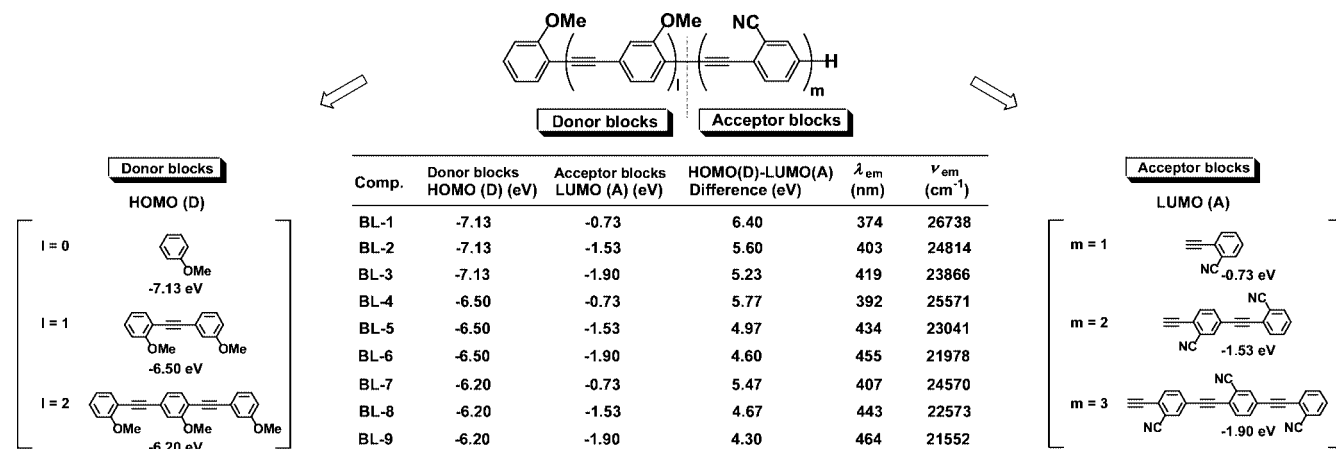
The observed solvent polarity effect on emission characteristics of BL systems suggests a considerable increase in the dipole moments at the excited-state (μ_e) compared with those

TABLE 5: HOMO–LUMO Gaps by the DFT Method, and Calculated (TD-DFT and INDO/S) and Experimental Optical Gaps for BL Systems

compound	n	calcd (DFT and TD-DFT) ^a				CI ^b coefficient	calcd (INDO/S)	expt	$\Delta\lambda_{abs}$ (calcd – expt, nm)	
		HOMO (eV)	LUMO (eV)	HOMO–LUMO gap (eV)	λ_{abs} (nm)				TD-DFT	INDO/S
BL-1	0	-6.79	-0.75	6.04	302	0.94	329	326	-24	+3
BL-2	1	-6.73	-1.44	5.30	342	0.91	348	358	-16	-10
BL-3	2	-6.72	-1.80	4.92	364	0.84	358	370	-6	-12
BL-4	1	-6.36	-0.98	5.38	339	0.92	346	352	-13	-6
BL-5	2	-6.37	-1.49	4.88	371	0.87	361	380	-9	-19
BL-6	3	-6.37	-1.81	4.56	387	0.77	370	386	+1	-16
BL-7	2	-6.17	-1.09	5.08	361	0.90	358	365	-4	-7
BL-8	3	-6.18	-1.51	4.67	385	0.80	364	387	-2	-23
BL-9	4	-6.19	-1.80	4.38	397	0.68	371	392	+5	-21

^a Functional: BHandHLYP; basis set: cc-pVDZ. ^b CI coefficient for a HOMO–LUMO transition that is normalized as $\sum_{i,j} CI(i \rightarrow j)^2 = 1$ with $CI(i \rightarrow j)$ being the coefficient for a transition from the i th occupied orbital to the j th unoccupied one. ^c Solvent used: CHCl₃

SCHEME 2: HOMO(D), LUMO(A), and λ_{em} in BL Systems



at the ground-state (μ_g) of BL systems. This interpretation was confirmed by plotting the Stokes shift (cm^{-1}) against the solvent orientation polarizability (Δf); namely, we can get the change in dipole moment $\Delta\mu$ ($=\mu_e - \mu_g$) arising from transition from the ground-state to the S_1 state using the Lippert–Mataga equation (eq 1):

$$\bar{\nu}_A - \bar{\nu}_F = \frac{2}{hc} \left(\frac{\epsilon - 1}{2\epsilon + 1} - \frac{n^2 - 1}{2n^2 + 1} \right) \frac{(\mu_e - \mu_g)^2}{a^3} + \text{constant} \quad (1)$$

where $\bar{\nu}_A$ and $\bar{\nu}_F$ are the peaks (cm^{-1}) of the absorption and emission. h is Planck's constant, c is the speed of light, ϵ is the dielectric constant of the solvent, n is the refractive index of the solvent, and a is the molecular radius.

As shown in Figure 5, the slope for BL-6 and BL-8 is much larger than that of SD-4 and SA-4 systems, indicating that the change in dipole moment $\Delta\mu$ becomes quite large in block modification systems because SD-4, SA-4, BL-6 and BL-8 have almost the same molecular radius. The results were summarized in Table 4, from which the fluorescence of BL system is considered to have the high charge-transfer nature. It is

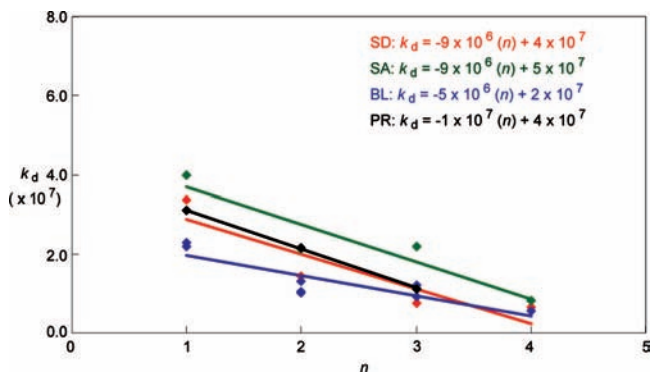


Figure 8. Relationship between k_d and n in SD, SA, BL and PR systems (except for $n = 0$).

considered that the interaction between solvent and BL systems in the S_1 state should be increased with increase in the solvent polarity, resulting in a decrease of Φ_f .

The high charge-transfer nature in the electronic transition of BL system is also suggested by the quantum chemical calculations with INDO/S, DFT, and TD-DFT methods. The

molecular orbitals calculated by the DFT method display a marked difference in the distribution of HOMO and LUMO in BL systems (Figure 6). Thus, charge-transfer transition from the HOMO to the LUMO is strongly suggested to occur in BL systems having longer π conjugation, because the HOMOs are wholly localized on the donor blocks, while the LUMOs are localized on acceptor blocks.

Some deviation ($\Delta\lambda_{\text{abs}}$) is seen in the optical gap between the calculations and the experimental observations by UV-vis spectroscopy (Table 5). In the short π -conjugated systems ($n = 0$ and 1), the values calculated by the INDO/S approach are in closer agreement with the experimental values than those for TD-DFT calculations using the BHandHLYP functional, while in the longer π -conjugated systems ($n = 2, 3$, and 4) the results are reversed. Although the TD-DFT wavelength values for BL systems are slightly smaller than the experimental values, the difference decreases with an increase in n value. The CI coefficient values imply that a HOMO-LUMO transition is predominant in the lowest energy transition.

The optical transition energy (ν_{em} ; cm^{-1}) from the S_1 state to the ground-state correlates linearly with the difference between the

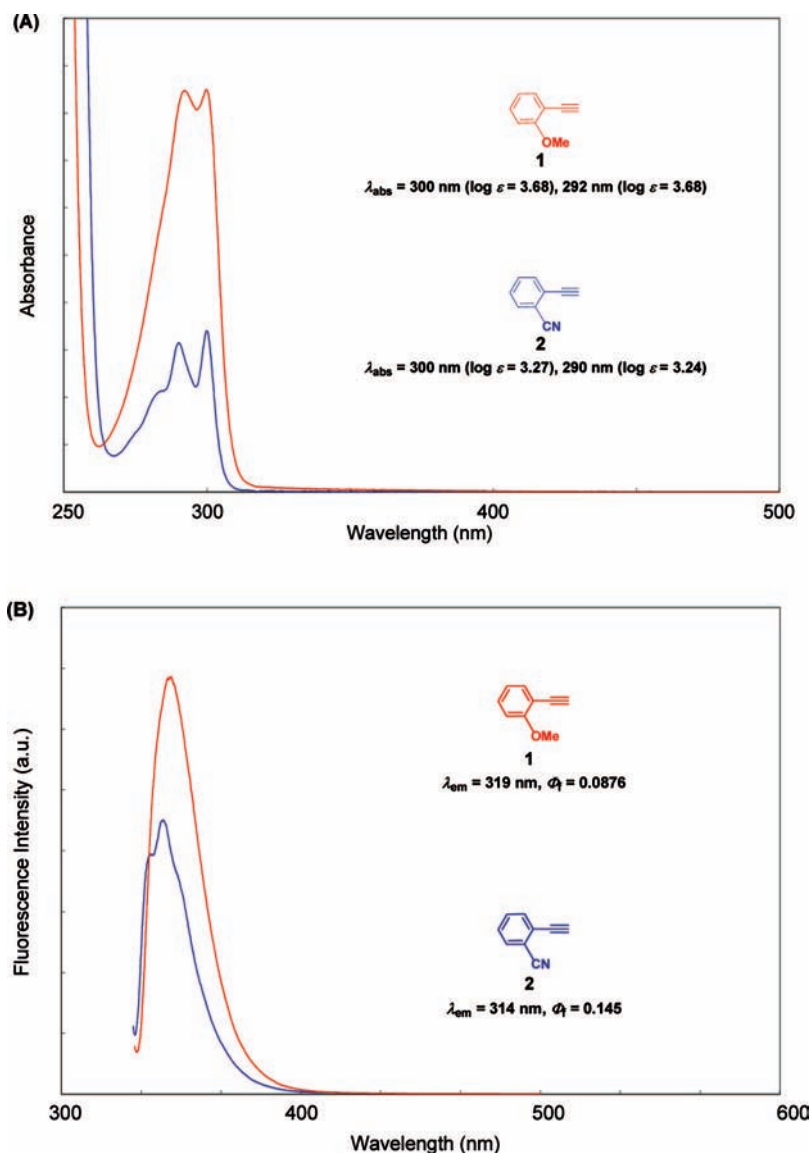
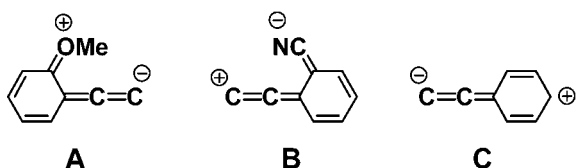


Figure 9. Absorption (A) and fluorescence (B) spectra of **1** (red) and **2** (blue) in chloroform.

HOMO of the donor blocks and the LUMO of the acceptor blocks (abbreviated as HOMO(D)–LUMO(A) difference) in **BL** systems, as shown in Scheme 2 and Figure 7. Therefore the fluorescence of **BL** systems is considered to have the high charge-transfer nature in the S_1 state as we already mentioned. The positive linear relationship between the optical transition energy (ν_{em} : cm^{-1}) from the S_1 state to the ground-state and the HOMO(D)-LUMO(A) difference should be of great interest.

3.3. The Relationship Between the Absolute Quantum Yield (Φ_f) and the Number (n) of EEDS Units. How the π conjugation length in the S_1 state effects the fluorescence emission is the heart of the matter in molecular and materials science. However, any practical method to estimate the π conjugation length in the S_1 state seems not to be reported except for our preliminary report.^{4c} We previously proposed a concept^{4b,e} in which the emission efficiency (Φ_f) depends on the number (n) of the EEDS in the S_1 state exemplified by A, B, and C in the present case, because the S_1 state is more polar than the ground state ($\mu_e > \mu_g$), as mentioned in the previous section. Although it is necessary to establish the generality of this concept by examination of various π conjugated systems, the n value of EEDS seems to be a measure of π conjugation length in the S_1 state, provided the S_1 state is coplanar.^{16,17}



This assumption can be supported by the linear relationship with negative slope between k_d and n , as shown in Figure 8, because k_d values relate to nonradiative rotational modes of the main chain and substituents. Namely, the k_d values linearly decrease with the n values, suggesting that the S_1 state planarity increases with the n values and the introduction of donor and/or acceptor groups.¹⁸ This is ascribable to the closing out of nonradiative rotational modes¹³ by the conjugative interaction of donor and/or acceptor groups with oligophenylene ethynylene

π skeletons and π delocalization in the skeleton in the S_1 state.^{19,20} It is considered that the slope of the linear correlation between λ_{em} and n (see Figure 10) may serve as a measure of coplanarity of **SD**, **SA**, and **BL** systems.

The energy migration¹⁶ between different dipolar structure units (**A** and **B**) in the block modification system is ascribed to their energetic equivalence, as indicated by the overlap of fluorescence and absorption spectra of **1** and **2**, as shown in Figure 9. Thus the sum of the number (l) of donor units and the number (m) of acceptor units becomes the n of EEDS for **BL** systems.

The positive linear relationship between λ_{em} and the n (≥ 1) of EEDS units for **SD**, **SA**, and **BL** systems (Figure 10) also supports our idea that the EEDS should be a measure of effective π conjugation length in the S_1 state. As seen in Figure 10, the block modification (**BL** systems) is more effective for the bathochromic shift of emission maximum judging from the ρ values: **BL** systems, 23.6 > **SD** systems, 16.2 > **SA** systems, 15.5).

To establish our concept that Φ_f depends on the n of EEDS units (π effective conjugation length) in the S_1 state, we examined the relationship between absolute quantum yield and number ($n > 1$) of the dipolar structures (**A**, **B**, and **C**). Consequently, we found that Φ_f linearly increases with n with a positive slope, as shown in Figure 11. It is really worth noting that a positive linear correlation is seen between Φ_f and the n of EEDS units. The slopes (ρ) for linear plots of Φ_f versus n show the contribution of EEDS units to the absolute quantum yield (Φ_f). As shown in Figure 11, ρ values decrease in the order of parent system (0.050), side donor modification system (0.044), and side acceptor modification system (0.038). It might be interesting to note that this order corresponds to that of the estimated dipole distance for the dipolar structure unit in the S_1 state (see Supporting Information). The intercept value 0.82 for the side donor modification system is close to the others, though very little difference is seen as follows: 0.80 for the side acceptor modification system, 0.84 for the block modification system, and 0.78 for the parent system. This linear relationship should be valuable for the creation of fluorophores with high light-emitting efficiency.

4. Conclusions

In conclusion, we created novel π -conjugated molecular rods modified by donor and/or acceptor groups (**SD-1**–**SD-**

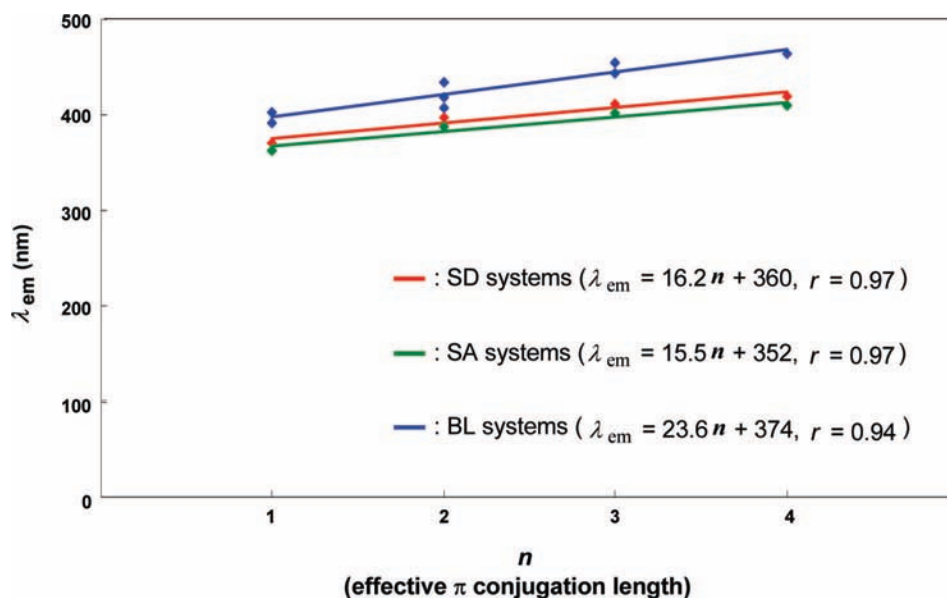


Figure 10. The relationship between λ_{em} and n in donor/acceptor modification systems (except for $n = 0$).

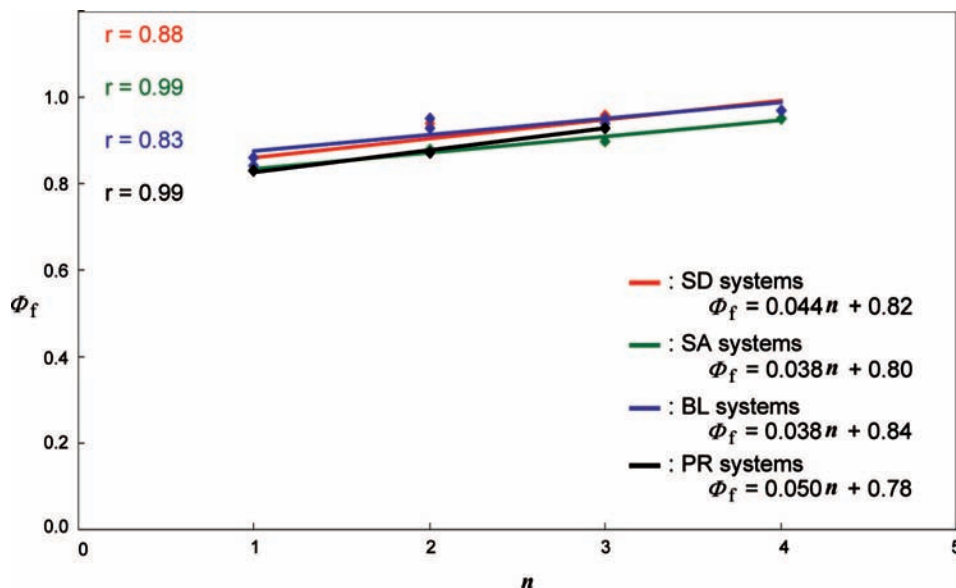


Figure 11. The relationship between absolute quantum yield (Φ_f) and the number (n) of the EEDS units (except for $n = 0$).

5, SA-1–SA-5, and BL-1–BL-9), and provided new physical chemistry insight by elucidating their fluorescence emission characteristics in solution and in solids, electronic and spectral features (in particular, the intramolecular charge transfer nature of S_1 state of BL systems) by means of solvent effect, Lippert–Mataga plot, and DFT and TD-DFT calculations. Finding a positive linear relationship between the optical transition energy (ν_{em} ; cm^{-1}) from the S_1 state to the ground-state and the HOMO(D)–LUMO(A) difference is of interest. From the positive linear relationship between λ_{em} and the n (≥ 1) of the EEDS unit, the n of the EEDS is regarded as a measure of the effective π -conjugation length in the S_1 state. The S_1 state planarity increase with the n of EEDS and the introduction of donor and/or acceptor groups. Thus highly fluorescent BL systems are created in which Φ_f values of BL-9 are close to unity. It is worth noting that the absolute quantum yield (Φ_f) increases linearly with the n of EEDS, which should be useful for the design of highly efficient fluorescent materials. It is suggested that solid-state emission intensity of BL systems could be enhanced by controlling the molecular orientation (face-to-face interaction) in solids and in crystals. Thus we have demonstrated that the block modification is most effective for the enhancement of fluorescence emission characteristics (increase in Φ_f and the bathochromic shift of λ_{em}) of rod-shaped π -conjugated carbon frameworks, which would provide a definable impact on the advancement of optoelectronic science and technology.

Acknowledgment. We thank professor M. Munakata (Kinki University) for single-crystal X-ray analysis of **1**. This work was supported by Grants-in-Aid for Creative Scientific Research (No. 16GS0209) and Scientific Research (No. 16550131) from the Ministry of Education, Culture, Sports, Science and Technology of Japan. Y.S. also acknowledges partial financial support from the Grant-in-Aid for Science Research in a Priority Area “Super-Hierarchical Structures” (17067018) from the Ministry of Education, Culture, Sports, Science and Technology of Japan.

Supporting Information Available: Spectral data for SD, SA, and BL systems, the energy differences between the two conformations (SD-1, SA-1, and BL-1), UV–vis and fluorescence spectra for BL systems, estimated dipole distance for A,

B, and C, schematic diagram for k_r and k_d , solvent effect on spectra, and X-ray structure and crystallographic data of **1**. This material is available free of charge via the Internet at <http://pubs.acs.org>.

References and Notes

- (1) (a) *Fluorescence Sensors and Biosensors*; Thompson, R. B., Ed.; CRC Press, LLC: Boca Raton, FL, 2006. (b) Nishioka, T.; Yuan, J.; Yamamoto, Y.; Sumitomo, K.; Wang, Z.; Hashino, K.; Hosoya, C.; Ikawa, K.; Wang, G.; Matsumoto, K. *Inorg. Chem.* **2006**, *45*, 4088. (c) Yoshimoto, K.; Nishizawa, S.; Minagawa, M.; Teramae, N. *J. Am. Chem. Soc.* **2003**, *125*, 8982. (d) Song, X.; Nolan, J.; Swanson, B. I. *J. Am. Chem. Soc.* **1998**, *120*, 11514. (e) *Biomedical Sensors, Fundamentals, and Applications*; Norton, N. H., Ed.; Noys Publications: Park Ridge, NJ, 1982.
- (2) (a) Shi, J.; Forsythe, E.; Morton, D. C.; Organic luminescent materials. U.S. Patent Application, 20,050,212,409, 2005. (b) *Organic Luminescent Materials*; Krasovitskii, B. M., Bolotin, B. M., Eds.; VCH: Weinheim, Germany, 1988.
- (3) (a) *Organic Light-Emitting Devices*; Shinar, J., Ed.; Springer: New York, 2004. (b) *Organic Light-Emitting Devices*; Müllen, K., Scherf, U., Ed.; Wiley-VCH: Weinheim, Germany, 2006.
- (4) For example, (a) Yamaguchi, Y.; Ochi, T.; Wakamiya, T.; Matsubara, Y.; Yoshida, Z. *Org. Lett.* **2006**, *8*, 717. (b) Yamaguchi, Y.; Kobayashi, S.; Wakamiya, T.; Matsubara, Y.; Yoshida, Z. *Angew. Chem., Int. Ed.* **2005**, *44*, 7040. (c) Yamaguchi, Y.; Tanaka, T.; Kobayashi, S.; Wakamiya, T.; Matsubara, Y.; Yoshida, Z. *J. Am. Chem. Soc.* **2005**, *127*, 9332. (d) Yamaguchi, Y.; Ochi, S.; Miyamura, T.; Tanaka, T.; Kobayashi, S.; Wakamiya, T.; Matsubara, Y.; Yoshida, Z. *J. Am. Chem. Soc.* **2006**, *128*, 4504. (e) Ochi, T.; Yamaguchi, Y.; Kobayashi, S.; Wakamiya, T.; Matsubara, Y.; Yoshida, Z. *Chem. Lett.* **2007**, *36*, 794.
- (5) Bunz, U. H. F. *Chem. Rev.* **2000**, *100*, 1605.
- (6) Fluorescent nonblock-type donor/acceptor OPEs; see (a) Wilson, J. N.; Bunz, H. F. *J. Am. Chem. Soc.* **2005**, *127*, 4124. (b) Marsden, J. A.; Miller, J. J.; Shircliff, L. D.; Haley, M. M. *J. Am. Chem. Soc.* **2005**, *127*, 2464. (c) Wilson, J. N.; Windscherf, P. M.; Evans, U.; Bunz, U. H. F. *Macromolecules* **2002**, *35*, 8681. (d) Nguyen, P.; Yuan, Z.; Agocs, L.; Marder, T. B. *Inorg. Chim. Acta* **1994**, *220*, 289.
- (7) Fukuzumi, S.; Ohkubo, K.; Suenobu, T.; Kato, K.; Fujitsuka, M.; Ito, O. *J. Am. Chem. Soc.* **2002**, *123*, 8459.
- (8) Frisch, M. J.; Trucks, G. W.; Schlegel, H. B.; Scuseria, G. E.; Robb, M. A.; Cheeseman, J. R.; Montgomery, J. A., Jr.; Vreven, T.; Kudin, K. N.; Burant, J. C.; Millam, J. M.; Iyengar, S. S.; Tomasi, J.; Barone, V.; Mennucci, B.; Cossi, M.; Scalmani, G.; Rega, N.; Petersson, G. A.; Nakatsuji, H.; Hada, M.; Ehara, M.; Toyota, K.; Fukuda, R.; Hasegawa, J.; Ishida, M.; Nakajima, T.; Honda, Y.; Kitao, O.; Nakai, H.; Klene, M.; Li, X.; Knox, J. E.; Hratchian, H. P.; Cross, J. B.; Bakken, V.; Adamo, C.; Jaramillo, J.; Gomperts, R.; Stratmann, R. E.; Yazyev, O.; Austin, A. J.; Cammi, R.; Pomelli, C.; Ochterski, J. W.; Ayala, P. Y.; Morokuma, K.; Voth, G. A.; Salvador, P.; Dannenberg, J. J.; Zakrzewski, V. G.; Dapprich, S.; Daniels, A. D.; Strain, M. C.; Farkas, O.; Malick, D. K.; Rabuck, A. D.; Raghavachari, K.; Foresman, J. B.; Ortiz, J. V.; Cui, Q.; Baboul, A. G.;

Clifford, S.; Cioslowski, J.; Stefanov, B. B.; Liu, G.; Liashenko, A.; Piskorz, P.; Komaromi, I.; Martin, R. L.; Fox, D. J.; Keith, T.; Al-Laham, M. A.; Peng, C. Y.; Nanayakkara, A.; Challacombe, M.; Gill, P. M. W.; Johnson, B.; Chen, W.; Wong, M. W.; Gonzalez, C.; Pople, J. A. *Gaussian 03, Revision C.02*; Gaussian, Inc.: Wallingford, CT, 2004.

(9) Sonogashira, K. In *Comprehensive Organic Synthesis*; Trost, B. M., Fleming, I., Eds.; Pergamon: Oxford, 1991; Vol. 3, pp 521–549.

(10) The compounds (**SD**, **SA**, **BL**, and **PR** systems) were purified by repeated column chromatography followed by recrystallization. Quite different from the usual case (purity checked by NMR, elemental analysis, etc.: 10^{-2} – 10^{-3} impurity), the purity of organic fluorescent compounds is not enough by these methods, and needs to be checked by the constancy of the fluorescence intensity at the maximum (λ_{em}) (10^{-6} – 10^{-7} impurity).

(11) (a) Leventis, N.; Rawashdeh, A.-M. M.; Elder, I. A.; Yang, J.; Dass, A.; Sotiriou-Leventis, C. *Chem. Mater.* **2004**, *16*, 1493. (b) *Principles of Photochemistry*; Barltrop, J. A., Coyle, J. D., Eds.; Wiley: New York, 1978; p 68.

(12) Saltiel, J.; Waller, A. S.; Sears, D. F., Jr.; Garrett, C. Z. *J. Phys. Chem.* **1993**, *97*, 2516.

(13) Sandros, K.; Sundahl, M.; Wennerstrom, O.; Norinder, U. *J. Am. Chem. Soc.* **1990**, *112*, 3082.

(14) (a) McFarland, S. A.; Finney, N. S. *J. Am. Chem. Soc.* **2002**, *124*, 1178. (b) Ishibashi, T.; Okamoto, H.; Hamaguchi, H. *Chem. Phys. Lett.*

2000, *325*, 212. (c) Hirata, Y. *Bull. Chem. Soc. Jpn.* **1999**, *72*, 1647. (d) Ishibashi, T.; Hamaguchi, H. *J. Phys. Chem. A* **1998**, *102*, 2263.

(15) Laurence, C.; Nicolet, P.; Dalati, M. T.; Abboud, J.-L. M.; Notario, R. *J. Phys. Chem.* **1994**, *98*, 5807.

(16) Polyarylene ethynylenes having side substitutes are reported to be coplanar in the ground-state until $n \leq 9$.¹⁷

(17) (a) Sluch, M. I.; Godt, A.; Bunz, U. H. F.; Berg, M. A. *J. Am. Chem. Soc.* **2001**, *123*, 6447. (b) Miteva, T.; Palmer, L.; Kloppenburg, L.; Neher, D.; Bunz, U. H. F. *Macromolecules* **2000**, *33*, 652.

(18) (a) Yang, J.-S.; Liau, K.-L.; Hwang, C.-M.; Wang, C.-M. *J. Phys. Chem. A* **2006**, *110*, 8003. (b) Pines, D.; Pines, D.; Retting, W. *J. Phys. Chem. A* **2003**, *107*, 236. (c) Lapouyade, R.; Czeschka, K.; Majenz, W.; Retting, W.; Gilabert, E.; Rulliere, C. *J. Phys. Chem.* **1992**, *96*, 9643. (d) Retting, W.; Majenz, W. *Chem. Phys. Lett.* **1989**, *154*, 335. (e) Gilabert, E.; Lapouyade, R.; Rulliere, C. *Chem. Phys. Lett.* **1988**, *145*, 262.

(19) Beeby et al. reported that π delocalization in the S_1 state is relatively small for **PR-2** (shorter PR system).²⁰ However, with increase in n value and the introduction of donor and/or acceptor groups, the delocalization is considered to be increased.

(20) Beeby, A.; Findlay, K. S.; Low, P. J.; Marder, T. B.; Matousek, P.; Parker, A. W.; Rutter, S. R.; Towrie, M. *Chem. Commun.* **2003**, 2406.

JP7113219